

Why the magnetic interactions in Na_xCoO_2 are 3D

M.D. Johannes,¹ I.I. Mazin,¹ and D.J. Singh²

¹Code 6391, Naval Research Laboratory, Washington, D.C. 20375

²Condensed Matter Sciences Division, Oak Ridge National Laboratory, Oak Ridge, TN 37831-6032

The puzzle of 3D magnetic interactions in the structurally 2D layered oxide Na_xCoO_2 is addressed using first principles calculations and analysis of the exchange mechanisms. The calculations agree with recent neutron results, favoring AFM stacking of FM planes. Superexchange via direct O-O hopping and through intermediate Na sp^2 hybrids couples each Co to its nearest and six *next-nearest* interplanar neighbors equally. The individual exchange constants are rather 2D, like the lattice itself, but due to multiple *c*-axis exchange paths, the magnetism becomes effectively 3D.

The layered transition metal oxide (TMO), Na_xCoO_2 is attracting considerable interest because of its unusual magnetic and transport properties, and the recently discovered superconductivity in its derivative, $\text{Na}_{1/3}\text{CoO}_2\cdot4/3\text{H}_2\text{O}$. Experimental signatures of triplet pairing^{2,3,4} have lead to suggestions that spin fluctuations^{5,6,7,8,9} mediate the superconductivity, in analogy with other layered superconducting TMO's like high- T_c cuprates and Sr_2RuO_4 , both of which are close to magnetic instabilities, as is Na_xCoO_2 .^{5,18} However, in contrast to those materials where not only the electronic structure, but also the magnetic interactions are strongly 2D, recent neutron measurements of the magnon dispersion^{19,20} in $\text{Na}_{x \approx 0.8}\text{CoO}_2$ indicate that the anti-ferromagnetic (AFM) exchange between CoO_2 planes is nearly as strong as the ferromagnetic (FM) in-plane exchange. Since dimensionality plays a key role in unconventional superconductivity, it is important to understand the microscopic physics behind the apparent 3D character of magnetic interactions observed in Refs. 19,20 and to clarify the relationship of the magnetic properties of the parent compound to those of the superconducting hydrate. We address these issues here.

Na_xCoO_2 has an unusual magnetic phase diagram as a function of x , which itself poses interesting, unresolved questions. For most x , Na_xCoO_2 is a metallic paramagnet, but in a very small range, around $x=0.5$, a charge-ordered, insulating, and possibly antiferromagnetic (AFM) region emerges¹⁰. Surprisingly, the metallic states on either side of this region are quite different. For $x < 0.5$ the susceptibility is Pauli paramagnet like with weak T dependence, while for $x > 0.5$ it is Curie-Weiss like, suggesting local moments. Finally, for x greater than ~ 0.75 a spin density wave condenses,^{11,12,13,14} with clear antiferromagnetism, $T_N \sim 22\text{K}$ at $x=0.82$. While this and the negative Weiss constant^{1,11,15,16} suggest antiferromagnetic interactions, experiments also show a characteristically ferromagnetic hysteresis¹¹ as well as predicted⁵ in-plane ferromagnetic fluctuations¹⁷.

These varied data are reconciled by neutron scattering experiments,^{19,20} which attribute the $T_M=22\text{K}$ transition to an A-type AFM ordering (FM planes stacked antiferromagnetically along the *c*-axis). By fitting magnon dispersion curves to a linear spin wave model, both groups conclude that in-plane and perpendicular magnetic ex-

change constants are of comparable magnitude, indicating magnetic isotropy, despite considerable structural two-dimensionality. We will show here that this quasi-isotropy does not imply comparable magnitudes of the nearest neighbor exchange constants in- and out-of-plane, but rather unexpectedly large coupling to next nearest neighbors across the planes, assisted mainly by Na sp^2 hybrid orbitals.

Our first principles local density approximation (LDA) calculations were done using the augmented plane wave plus local orbital (APW+lo) and linearized augmented planewave (LAPW) methods implemented in two codes.^{21,22} The experimental lattice parameters, $a=2.828\text{\AA}$, $c=10.94\text{\AA}$, and LDA relaxed oxygen height $z_{\text{O}}=0.0859$ were used for all calculations.²³ The partial occupation of Na was treated both by the virtual crystal approximation (VCA) and in supercells. In the VCA, each $2d$ Wyckoff position of the $P6_3/mmc$ cell was occupied by a fictitious atom, atomic number, $Z = 10 + x$, to model a partial occupancy of x . We also did some calculations with Na at the $2b$ positions. Supercell calculations were done at selected x with real Na at some $2d$ or $2b$ positions.

Prior calculations show that there is a FM solution in the LDA¹⁸ for Na_xCoO_2 for all x in the experimentally relevant range. Our calculations for a tripled $x = 2/3$ supercells show that the A-type AFM order recently revealed by neutrons is actually the preferred LDA ground state. AFM stacking of the ferromagnetic layers is favored by 2.3 meV/Co for Na in the $2b$ site (Na on top of Co) in a $\sqrt{3} \times \sqrt{3}$ supercell, and 1.7 meV/Co in the $2d$ site. This is consistent with a recently measured²⁴ metamagnetic AFM to FM transition at the relatively low field of 8T. We find very similar results in the VCA: 1.4 meV/Co with Na in site $2d$ and 2.2 meV/Co with Na in site $2b$. The total spin moment inside the Co APW spheres for the A-type AFM ordering is only $\sim 0.02 \mu_B$ less than that in the FM case which is half metallic. In other words, the Co is maximally spin polarized for the doping level x consistent with the $\sim 0.2 \mu_B$ limit from neutron²⁵ and muon spin relaxation¹² experiments at $x \sim 0.8$. However, note that at $x = 2/3$, samples are paramagnetic; the LDA ordered ground state is presumably suppressed by quantum critical fluctuations that are potentially important for superconductivity.⁵

We now turn to the relative magnitude of in-plane and perpendicular exchange constants. Since the band structure is metallic, antiferromagnetic superexchange competes with ferromagnetic double exchange (the former depends on hopping linearly, and the latter quadratically). The large in-plane dispersion leads to a net FM in-plane interaction, while the net inter-plane coupling, due to the smaller c -axis dispersion, is AFM. As mentioned, nearly isotropic 3D magnetic interactions are unexpected in layered compounds. Still this is not inconsistent considering the large bonding-antibonding splitting of the a_{1g} band in LDA calculations²⁶ at large x . At $x=2/3$, this splitting at Γ is 0.21 eV, i.e. 15% of the full t_{2g} bandwidth. If the band structure is mapped onto an effective Co-only model and only nearest neighbor hopping across the planes is allowed, as assumed in Refs. 19 and 20 (we will argue that this is *not* a good approximation), and the effective hopping amplitude is t_{\perp} , then the a_{1g} splitting at Γ would be $12t_{\perp}$ and there would be no first order splitting for the two e'_g bands (consistent with the LDA band structure). This gives $t_{\perp} \approx 15$ meV. Although the $t_{2g} - t_{2g}$ in-plane hopping is nearly an order of magnitude larger, this still gives less anisotropy than would be anticipated for a layered material.

To proceed, we need to understand the physics of the interlayer coupling. The hopping must proceed, via O p states, which, in turn, requires either direct O $p_z - p_z$ hopping or hopping assisted by diffuse unoccupied Na s and p orbitals. In the latter case the details of Na placement may be important. Moreover, it is significant that the energy separation between the unoccupied Na $3s$ and $3p$ states in Na_xCoO_2 is found to be rather small, smaller in fact than the corresponding band width. This allows the s and $p_{x,y}$ orbitals of a Na atom, sitting inside an O₆ prism, to combine and form bands that may be described as coming from sp^2 hybrid orbitals, specifically, $h_1 = (s - \sqrt{2}p_y)/\sqrt{3}$, $h_{2,3} = (s \pm \sqrt{3/2}p_x + p_y/\sqrt{2})/\sqrt{3}$. These are asymmetric, orthonormal, and directed to the midpoints of the O prism edges. So the Na-assisted part of the O-O hopping goes from one O to another O above it via one, two, or three Na sp^2 hybrids depending on how many of the three nearby Na sites are occupied. Note that if only Na s states were involved, the hopping amplitude to a second nearest neighbor O in the next plane via a specific Na atom would be the same as that of hopping to the O right on top. Thus Na p participation changes the interlayer coupling in an essential way.

Besides the Na assisted hopping, direct O-O hopping may be important. Considering the rhombohedral O site symmetry, the relevant hopping is from Co a_{1g} to O p_z . Further, in Na_xCoO_2 , the O atoms in adjacent CoO₂ sheets are directly on top of each other, favoring interlayer hopping via the opposing O p_z orbitals. To estimate this contribution we suppressed the Na-assisted hopping in three ways. First, we looked at $\text{CoO}_2 + x e^-$ i.e., a compound without Na, but with the correct number of valence electrons compensated by a uniform background charge. At $x = 2/3$, the resulting a_{1g} band-

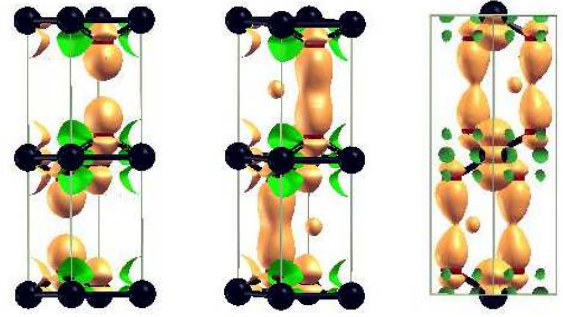


FIG. 1: (color online) Charge density of the a_{1g} bonding orbital in $\text{X}_{2/3}\text{CoO}_2$ with $\text{X} = e^-$ (left), $\text{X} = \text{VCA Na}$ (middle), and $\text{X} = \text{real Na}$ (right). The Na ions facilitate O-O bonding and thus superexchange. The VCA and supercell calculations differ in the asymmetry of the sp^2 hybrid.

splitting at Γ is 0.12 eV or $\approx 70\%$ of the total effective coupling in $\text{Na}_{2/3}\text{CoO}_2$. We verified that this is independent of the amount of extra valence charge in the system, by doing calculations with 0.82, 0.75, and 0.4 extra e^- . Next, for $x = 2/3$, we put Ne in the Na sites, again adding electrons with a compensating background. Finally, we did calculations for $\text{Na}_{2/3}\text{CoO}_2$, where Na denotes Na with s and p orbitals artificially shifted to higher energy. The results change very little, indicating that the splitting from direct O-O hopping is ~ 0.12 eV. Thus, the effective interplanar coupling can be written as $t_{\perp} = t_{\perp}^{Na}(x) + t_{\perp}^O$, where $t_{\perp}^{Na}(x)$ is a function of doping and t_{\perp}^O is constant, and $t_{\perp}^{Na}(x)/t_{\perp}^O$ varies from 0.48 to 0.78 in the range $0.6 \lesssim x \lesssim 0.9$.

The Na assisted hopping can be assessed using VCA or supercell calculations. These differ in two ways. First, in the VCA, all Na sites are occupied regardless of x , while in a supercell and in reality a portion, $1 - x$ are empty. The number of effective hopping paths via Na, and, correspondingly, the effective hopping between the planes, should therefore be reduced in this proportion relative to the VCA. Second, the VCA nuclear charge is $Z = 10 + x$, so the unoccupied Na s and p energies are moved up. This will reduce the Na-O hybridization, which is inversely proportional to the energy separation between Na $3s(p)$ and O $2p$ bands. This implies an artificial monotonic increase of Na-assisted hopping with x in the VCA. These two effects are in opposite directions and should at least partially cancel. To assess this, we performed VCA calculations for $0 \leq x \leq 1$, and supercell (real Na) calculations for $x=0, 1/2, 2/3$ and 1. The calculated VCA a_{1g} splitting at Γ depends on x non-linearly in both cases; the supercell calculations give similar results with slightly larger splittings. (Fig. 2). We verified that the deviation from this linearity for the supercell calculations has the same origin as in the VCA: the Na $3s$ and $3p$ levels shift with x though to a lesser degree than in the VCA (the shift is due to the changing Coulomb potential as a function of doping). This is seen in the charge density of the bonding a_{1g} state at Γ , (Fig. 1).

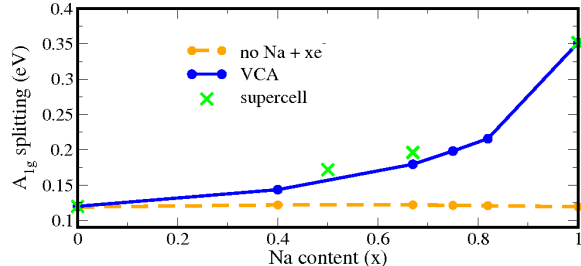


FIG. 2: A comparison of VCA and supercell a_{1g} splitting at the Γ point, with the same structural parameters(see text), showing a monotonic increase with x . Calculations without Na orbitals, but with the proper valence charge show that the O-O hopping contribution is independent of x .

The relatively weak O $p_z - p_z$ overlap is augmented in the VCA by a composite state in the middle of the O-O bond, consisting of the three Na sp^2 hybrids; removal of one of these with the corresponding Na atom in the $Na_{2/3}CoO_2$ supercell makes the O orbitals tilt towards the remaining Na ions.

A somewhat counterintuitive consequence of the above analysis is the fact that the nearest neighbor approximation is invalid for inter-plane hopping. Neither a Co-O-Na-O-Co path nor a Co-O-O-Co path needs to end on the Co site directly above the one where it started. There are 9 different Na-containing paths connecting nearest neighbor Co ions in different planes²⁷, and 3 connecting one Co with each of the 6 second neighbors²⁸. For paths without Na, there are 3 that connect nearest neighbors and 1 that connects second neighbors. Assuming that each Na-containing path contributes τ to the effective interplanar hopping amplitude and each O-only path contributes τ' , we find that $t_{\perp}^{Na}(x, \mathbf{k})/t_{\perp}^O(\mathbf{k}) = 3\tau x/\tau'$ and

$$t_{\perp}^O(\mathbf{k}) = \tau'(3 + 2 \cos \mathbf{a}\mathbf{k} + 2 \cos \mathbf{b}\mathbf{k} + 2 \cos \mathbf{c}\mathbf{k}), \quad (1)$$

where \mathbf{a} , \mathbf{b} , and \mathbf{c} are respectively the three projections onto the ab plane of the vectors connecting a given Co ion with the three O above. At Γ , $t_{\perp}^{Na} = 27\tau x$, and $t_{\perp}^O = 0.12$ eV, thus we find, at $x=0.82$, $\tau = 0.5$ meV and $\tau' = 1.1$ meV. Finally, we use the number of τ and τ' paths that connect a Co ion to each type of neighbor to calculate t_c and t'_c , the hopping integrals for first and second Co interplanar coupling to get:

$$\frac{J_c}{J'_c} = \frac{t_c^2}{t'_c^2} = \left(\frac{9\tau \cdot x + 3\tau'}{3\tau \cdot x + \tau'} \right)^2 = 9 \quad (2)$$

We now revisit the interpretation of the spin wave dispersion observed in Refs. 19 and 20, including second neighbor assisted hopping. A straightforward generalization of Eq. 2 in Ref. 19 yields

$$E = 2S \sqrt{\{\tilde{\mathcal{J}}_{\perp}(0) - \mathcal{J}_{\parallel}(0) + \mathcal{J}_{\parallel}(\mathbf{q}) + (\frac{D}{2S})\}^2 - \{\tilde{\mathcal{J}}_{\perp}(\mathbf{q})\}^2}$$

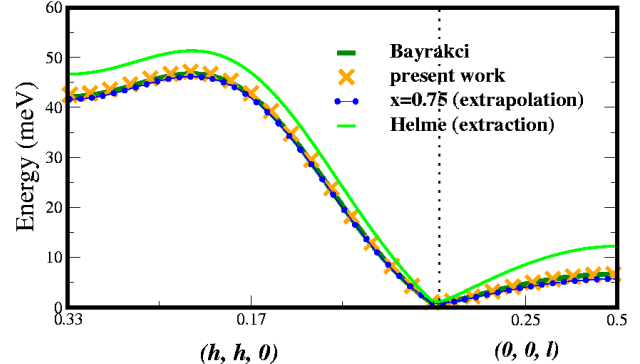


FIG. 3: Magnon dispersion of Na_xCoO_2 along high symmetry lines shown for $x= 0.7$ and $x=0.82$. The results of two experiments in which data were fit to a nearest-neighbor interaction model are compared to our dispersion which includes second-nearest out-of-plane neighbors. Our parameters were fit to the data of Ref. 19 for $x=0.7$, adjusted for Na content (see text), and used to get the dispersion for $x=0.82$ without re-fitting.

where, following their notation, hkl is the wave vector in units of the reciprocal lattice vector. $\tilde{\mathcal{J}}(\mathbf{q}) = \mathcal{J}_c(\mathbf{q}) + \mathcal{J}'_c(\mathbf{q})$ and $\mathcal{J}'_c(\mathbf{q}) = 2J'_c \cos(\pi l)[2 \cos(2\pi h) + 2 \cos(2\pi k) + 2 \cos(2\pi(h+k))]$. Using the $\mathbf{k} = (0, 0, 1/2)$ magnon energy, we can extract $J_c = 1.98$ meV and $J'_c = 0.22$ meV. This fits experiment¹⁹ well with $J_{\parallel} = -4.5$ meV. Bayrakci *et al*, using nearest neighbors only, found $J_c = 3.3$ meV and $J_{\parallel} = -4.5$ meV, leading to the conclusion of magnetic isotropy. Fig. 3 shows that our model produces results that are completely indistinguishable from the nearest neighbor model used in Ref. 19, however, the parameters are more physically reasonable and compatible with the highly anisotropic electronic structure of the compound.

Finally, we address the differences in the magnon dispersions obtained in Ref. 19 and Ref. 20, both shown in Fig. 3. Because of notational differences between Ref. 19 and Ref. 20, we extract exchange constants directly from the Ref. 20 data, using the same formalism as Ref. 19 and get $J_c = 6.1$ eV and $J_{\parallel} = -4.5$ eV. Using VCA calculations at $x=0.7$ and $x=0.82$, we scale the parameters of our nearest and next-nearest neighbor model and compare them with the results of Helme *et al.*²⁰ We estimate that at $x = 0.75$ $J_c = 1.69$ meV, $J'_c = 0.19$ meV, and $J_{\parallel} = -4.5$ meV. So, the in-plane hopping remains unchanged, in agreement with experiment, and the interplanar hopping decreases by $\approx 8\%$, since less Na is available to mediate it.

The measured dispersion²⁰ in the z direction is much larger at $x=0.75$ than at $x=0.82$. Other effects, not accounted for here, must therefore be operative. One possibility is a different pattern of Na ordering. Indeed, in our $x = 2/3$ supercell calculations placing all the Na at the $2b$ sites instead of the $2d$ sites yields a $\sim 35\%$ increase in the interlayer coupling. While this number no doubt depends on the exact Na arrangement, it does indicate

sensitivity to the ordering of a size sufficient to explain the experiment. In comparing with experiment, it should be also noted that Co disproportionation, seen by NMR studies²⁹ around $x=0.7$, would change the spin arrangement of the lattice and therefore the magnon dispersion. Co ions with formal valency $(4-x)^+$ split proportionally into non-magnetic Co^{3+} and $S = 1/2 \text{Co}^{4+}$. The particular arrangement is unknown, but the exchange interaction may be changed. Note that the phase boundary of charge order is not yet clearly defined and calculations³⁰ suggest that, near the crossover, there is a region where two distinct magnetic ions exist. Another consideration is that the spin-wave model adopted here and in Refs. 19 and 20 assumes a rigid spin moment of $S=1/2$, which may not be a good approximation for the weak magnetism in this compound. The actual moment, both measured and calculated, is smaller and grows with x . Last but not least, one should keep in mind that FM and AFM interactions here are competing with each other thereby amplifying the relative effect of doping changes on magnetism.

In summary, we find that inter-plane coupling to second neighbors plays an important role in the out-of-plane magnetism of Na_xCoO_2 . Heisenberg type models including only one nearest neighbor exchange across the plane are insufficient; exchange between the six next nearest neighbors in adjacent planes is needed. Fortunately, one can estimate the ratio of the two exchange constants,

making it possible to extract them from experiment without increasing the number of fitting parameters. The resulting exchange constants provide a magnon spectrum that matches experiment extremely well and yields a physically realistic picture of magnetic interactions in this layered material. The LDA energy difference between the FM and the A-type AFM ordering for Na content $x = 2/3$ is ~ 2 meV/Co, which is reasonable considering the exchange coupling deduced from experimentally measured spin wave dispersion (6.6 meV and 12.1 meV/Co in Refs. 19 and 20, respectively). We note that superexchange drops with the distance more strongly than other coupling mechanisms, such as double exchange. Thus, although the inter-planar coupling is surprisingly strong in Na_xCoO_2 , yielding three dimensional magnetic character, it would be expected to be very weak in the hydrated superconducting compound. It is even possible that a cross-over from AFM to FM coupling occurs with hydration due to suppression of the superexchange interaction. If the magnetic interactions become effectively 2D in the hydrated compound, fluctuations would be enhanced, possibly revealing superconductivity associated with a nearby magnetic quantum critical point.

We are grateful for helpful discussions with A.T. Boothroyd, R. Jin and S. Nagler. Work at Oak Ridge National Laboratory is supported by the U.S. Department of Energy.

¹ Y. Wang *et al*, *Nature* **423**, 425 (2003).
² W. Higemoto *et al*, *Phys. Rev. B* **70**, 134508 (2004).
³ A. Kanigel *et al*, *Phys. Rev. Lett.* **92**, 257007 (2004).
⁴ T. Waki *et al*, *cond-mat/0306036* (2003).
⁵ D. J. Singh, *Phys. Rev. B* **68**, 020503 (2003).
⁶ M. D. Johannes, I. I. Mazin, D. J. Singh, and D. A. Papaconstantopoulos, *PRL* **93**, 097005 (2004).
⁷ K. Ishida *et al*, *J. Phys. Soc. Jpn.* **72**, 3041 (2003).
⁸ A. Tanaka and X. Hu, *Phys. Rev. Lett.* **91**, 257006 (2003).
⁹ T. Fujimoto *et al*, *Phys. Rev. Lett.* **92**, 047004 (2004).
¹⁰ M. L. Foo *et al*, *Phys. Rev. Lett.* **92**, 247001 (2004).
¹¹ T. Motohashi *et al*, *Phys. Rev. B* **67**, 064406 (2003).
¹² J. Sugiyama *et al*, *Phys. Rev. B* **67**, 214420 (2003).
¹³ B. C. Sales *et al*, *Phys. Rev. B* **70**, 174419 (2004).
¹⁴ J. Wooldridge, D. M. Paul, G. Balakrishnan, and M. R. Lees, *cond-mat/0406513* (2004).
¹⁵ J. L. Gavilano *et al*, *cond-mat/0308383* **69**, 100404 (2004).
¹⁶ F. C. Chou, J. H. Cho, and Y. S. Lee, *Phys. Rev. B* **70**, 144526 (2004).
¹⁷ A. T. Boothroyd *et al*, *Phys. Rev. Lett.* **92**, 197201 (2003).
¹⁸ D. J. Singh, *Phys. Rev. B* **61**, 13397 (2000).
¹⁹ S. P. Bayrakci *et al*, *cond-mat/0410224* (2004).
²⁰ L. M. Helme *et al*, *cond-mat/0410457* (2004).
²¹ We did well converged calculations with the Wien2k code²²

and an independent LAPW code. These gave practically identical results when tested for the same system. For the APW+lo calculations sphere radii of $1.9 a_0$, $1.6 a_0$ and $2.0 a_0$ were used for Co, O and Na, respectively. For the LAPW calculations the corresponding radii were $1.95 a_0$, $1.55 a_0$ and $2.0 a_0$.
²² P. Blaha, K. Schwarz, G. K. H. Madsen, D. Kvasnicka, and J. Luitz, *Wien2k* (2002), ISBN 3-9501031-1-2.
²³ We verified that relaxing the O position as a function of x has relatively little effect, and keeping the position fixed helps elucidate the physics related to Na doping.
²⁴ J. L. Luo *et al*, *Phys. Rev. Lett.* **93**, 187203 (2004).
²⁵ S. P. Bayrakci *et al*, *Phys. Rev. B* **69**, 100410 (2004).
²⁶ M. D. Johannes, D. A. Papaconstantopoulos, D. J. Singh, and M. J. Mehl, *Euro. Phys. Lett.* **68**, 433 (2004).
²⁷ Note that if hopping was only via Na s orbitals, and not Na sp² hybrids, this counting would be different.
²⁸ This is independent of whether the Na is at the $2b$ or the $2d$ sites.
²⁹ I. R. Mukhamedshin, H. Alloul, G. Collin, and N. Blanchard, *Phys. Rev. Lett.* **93**, 167601 (2004).
³⁰ K. -W. Lee, J. Kunes, and W. E. Pickett, *Phys. Rev. B* **70**, 045104 (2004).